Proteomic Analysis of Mouse Testis Reveals Perfluorooctanoic Acid-Induced Reproductive Dysfunction via Direct Disturbance of Testicular Steroidogenic Machinery

Hongxia Zhang,[§,#] Yin Lu,[§,#] Bin Luo,[§,‡] Shengmin Yan,[§] Xuejiang Guo,[†] and Jiayin Dai*[,§]

[§]Key Laboratory of Animal Ecology and Conservation Biology, Institute of Zoology, Chinese Academy of Sciences, Beijing, 100101, P.R. China

[‡]School of Life Science, Anhui University, Hefei, 230601, P.R. China

[†]State Key Laboratory of Reproductive Medicine, Nanjing Medical University, Nanjing, 210029, P.R. China

S *Supporting Information*

ABSTRACT: Perfluorooctanoic acid (PFOA) is a ubiquitous environmental pollutant suspected of being an endocrine disruptor; however, mechanisms of male reproductive disorders induced by PFOA are poorly understood. In this study, male mice were exposed to 0, 0.31, 1.25, 5, and 20 mg PFOA/kg/day by oral gavage for 28 days. PFOA significantly damaged the seminiferous tubules and reduced testosterone and progesterone levels in the testis in a dose-dependent manner. Furthermore, PFOA exposure reduced sperm quality. We identified 93 differentially expressed proteins between the control and the 5 mg/kg/d PFOA treated mice using a quantitative proteomic approach. Among them, insulin like-factor 3 (INSL3) and cytochrome P450 cholesterol side-chain cleavage enzyme (CYP11A1) as Leydig-cell-specific markers were significantly decreased. We examined in detail the expression patterns of CYP11A1 and associated genes involved in steroidogenesis in the mouse testis. PFOA inhibited the mRNA and protein levels of CYP11A1 and the mRNA levels of 17β-hydroxysteroid dehydrogenase (17β-HSD) in a dose-dependent manner. Moreover, *in vitro* study showed the reduction in progesterone levels was accompanied by decreased expression of CYP11A1 in cAMP-stimulated mLTC-1 cells. Our findings indicate that PFOA exposure can impair male reproductive function, possibly by disturbing testosterone levels, and CPY11A1 may be a major steroidogenic enzyme targeted by PFOA.

KEYWORDS: *perfluorooctanoic acid, iTRAQ, male rats, testis, CYP11A1*
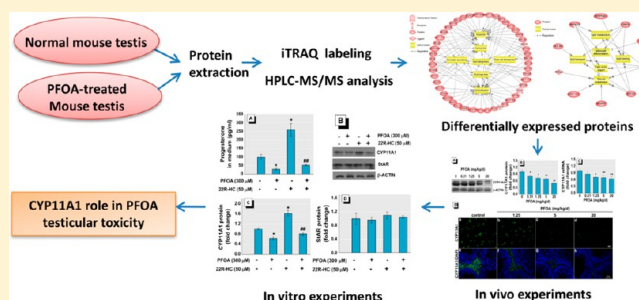
INTRODUCTION

Perfluorinated carboxylic acids (PFCAs), such as ammonium salts of perfluorooctanoic and perfluorononanoic acid (PFOA and PFNA), are synthetic compounds with an annual production of several hundred metric tons per year since the 1950s.[1] They have been widely applied in various industries and consumer products, especially as surfactants to make water- and oil-resistant products.[2] The strong carbon−fluorine bond in PFCAs contributes to their wide application but also results in a high degree of environmental persistence and bioaccumulation. Perfluorooctanoic acid (PFOA) is the most well-known and abundant PFCA in the environment.[3] In addition to its frequent presence in the ambient environment, PFOA is consistently detectable in the serum of wildlife and humans.[4−6] The highest levels of PFOA in humans have been reported in ammonium perfluorooctanoate production workers, with serum PFOA concentrations of 114,100 ng/mL.[7] Although PFOA does not accumulate in fatty tissues due to its lipophobic and hydrophobic chemical properties, it is a protein-binding PFCA, with a serum half-life of 16−22 days in mice[8] and 2−4 years in humans.[9]

Due to its extensive application and high bioaccumulation, PFOA toxicity has received wide attention. Classic toxicological studies in adult animals have suggested that PFOA causes liver hypertrophy and a common tumor triad consisting of hepatocellular carcinomas, pancreatic acinar cell tumors, and Leydig cell tumors.[10,11] PFOA is also a potential endocrine disruptor,[12] and the effects of PFOA on the male reproductive system have been evaluated in animal models, including the reduction in serum testosterone levels and increase in estradiol levels in rodents,[13,14] estrogen-like responses and disruption of gonad development in fish,[15,16] and changes in steroidogenic enzyme activities in humans and rats.[13,14,16,17] Testicular toxicities of other PFCAs, such as PFNA (C9) and perfluorododecanoic acid (PFDoA, C12) have also been studied.[18−20] In regards to human epidemiology, recent findings suggest that exposure to PFOA may help account for the otherwise unexplained poor semen quality observed in many young men today.[21] Vested et al.[22] also reported that *in*

utero exposure to PFOA was associated with lower sperm concentration and total sperm count; however, another recent study evaluated semen quality among 256 infertility patients in relation to perfluorooctanesulfonate (PFOS) and PFOA in serum and semen and found no association between PFOA levels and sperm concentration, volume, or motility.[23] Since these epidemiological data are inconsistent, testicular toxicity of PFCAs, especially that of PFOA, and the mechanism of action need further exploration.

Proteomic technologies have been successfully used in the toxicology field, with isobaric tags for relative and absolute quantitation (iTRAQ) one of the most widely used approaches. The advantage of iTRAQ is the simultaneous identification and quantification of proteins differentially expressed between experimental and control specimens and the exhibition of a large dynamic range in profiling both high and low abundance proteins. In addition, it can simultaneously analyze four to eight different specimens, thus increasing throughput while reducing experimental error. In this study, using iTRAQ combined with two-dimensional liquid chromatography and tandem mass spectrometry (2DLC−MS/MS), we identified the differentially expressed proteins in the male mouse testis after PFOA exposure. To our knowledge, this is the first study to investigate proteomic changes in relation to the testicular toxicity of PFOA using iTRAQ. Histopathological examination, hormone and lipid levels, and steroidogenic gene expression levels in the testis were also determined. These data will provide novel insight into the molecular mechanisms involved in the testicular toxicity of PFOA.

■ EXPERIMENTAL PROCEDURES

Chemicals and Animal Treatment

Perfluorooctanoic acid (PFOA, 96% purity), 22R-hydroxycholesterol (22R-HC), adenosine 3′,5′-cyclic monophosphate (cAMP), 3-(4, 5-dimethylthiazol-2-yl)-2,5-diphenyl tetrazolium bromide (MTT), and trypan blue were purchased from Sigma-Aldrich (St. Louis, MO). The chemicals used in LC−MS/MS were of HPLC grade, and all other chemicals used were of analytical grade.

Male BALB/c mice (age 6−8 weeks) were obtained from the Weitong Lihua Experimental Animal Center (Beijing, China). All experimental manipulations were performed in accordance with the Institutional Guidelines for the Care and Use of Laboratory Animals. Mice were housed in a mass air displacement room with a controlled environment (12:12 h light:dark cycle, 20−26 °C and 40−60% relative humidity). Food and water were provided *ad libitum* throughout the study. After 1 week of adaptation, 80 mice were randomly divided into five groups of equal size and dosed by oral gavage with either vehicle (Milli-Q water) or PFOA (dissolved in Milli-Q water) at 0.31, 1.25, 5, or 20 mg/kg/d for 28 consecutive days. The doses of PFOA were chosen according to an earlier toxicological study.[24] After treatment, all mice and their testes in both sides were weighed. Five mice from the control group and five mice from the 5 mg/kg/d group were randomly taken for sperm analysis. Details of this analysis are given in Supporting Information (SI). The remaining mice were sampled for other analyses. The right testes of three mice were fixed in 10% Bouin's fixative for histological examination, while the remaining testes were immediately frozen in liquid nitrogen and stored at −80 °C. This study was approved by the Animal Ethics Committee of the Institute of Zoology, Chinese Academy of Sciences (ID: IOZ14048).

PFOA Extraction and Analysis

Three testes samples in each group were selected randomly to determine PFOA concentrations. Testes were extracted with 5 mL of acetonitrile (ACN) in a 15 mL polypropylene (PP) tube, with all tubes placed on a mechanical shaker for 20 min and then centrifuged at 3000 × g for 10 min. The extract was subjected to further purification using the SPE-Oasis-WAX-method (details in SI).

Sample extracts were analyzed by high performance liquid chromatography−tandem mass spectrometry (HPLC−MS/MS) as described by Bao et al.[25] Chromatography was performed by an Agilent 1100 HPLC system with an Agilent Eclipse Plus C18 column (2.1 mm × 100 mm, 3.5 μm) (Agilent Technologies, Palo Alto, CA). The HPLC system was interfaced to an Agilent 6410 Triple Quadrupole (QQQ) mass spectrometer (Agilent Technologies, Santa Clara, CA) operated with electrospray ionization (ESI) in negative mode. Details on the parameters and quality control for PFOA analysis are described in the SI and previous research.[25]

Protein Preparation, iTRAQ Labeling and Strong Cationic Exchange (SCX) Fractionation

Three individual freeze-dried testes samples from the control and three samples taken from the 5 mg PFOA/kg/d group were randomly selected for iTRAQ analysis based on the histopathological examination and body weight results. Each weighed sample was added to 500 μL of lysis buffer (7 M urea, 2 M thiourea, 4% CHAPS, 40 mM Tris-HCl, pH 8.5) containing 1 mM of phenylmethylsulfonyl fluoride (PMSF), 2 mM of EDTA, and 10 mM of DTT, lysed by sonication and then centrifuged at 25,000 × g for 20 min at 4 °C. The collected supernatant was stored at −80 °C for subsequent iTRAQ and Western blot analysis. The protein concentration of each sample was measured using the Bradford assay.

iTRAQ labeling was done according to the kit protocol (ABI, Foster City, U.S.A.). One hundred micrograms of each extract were reduced, alkylated, and then precipitated using acetone at −20 °C. The precipitates were suspended in 20 μL of 0.5 M triethylammonium bicarbonate (TEAB) (Applied Biosystems, Foster City, U.S.A.) by sonication, and digested with trypsin (Promega, Madison, WI, U.S.A.) at 37 °C overnight. The tryptic peptides in the three biological samples from the control and PFOA-treated groups were labeled with iTRAQ reagents (isobaric tags 113, 114, and 116 for the control, and 117, 119, and 121 for the treated group) (Applied Biosystems).

The labeled peptides were pooled and dried by vacuum centrifugation. SCX chromatography was performed with a Shimadzu LC-20AB HPLC pump system connected to a 4.6 mm × 250 mm Ultremex SCX column (Phenomenex USA). The peptide mixtures were reconstituted with 4 mL of buffer A (25 mM NaH$_2$PO$_4$ in 25% CAN, pH 2.7), and then eluted at a flow rate of 1 mL/min with a gradient of buffer A for 10 min, 5−35% buffer B (25 mM NaH$_2$PO$_4$, 1 M KCl in 25% ACN, pH 2.7) for 11 min, and 35−80% buffer B for 1 min. Elution was monitored by measuring the absorbance at 214 nm, and fractions were collected every 1 min. The eluted peptides were pooled into 12 fractions, desalted with a Strata X C18 column (Phenomenex), and vacuum-dried.

LC—ESI-MS/MS analysis

Mass spectroscopic (MS) analysis was performed using a Triple TOF 5600 mass spectrometer (AB SCIEX, Concord, ON) coupled with a nanoACQuity HPLC system (Waters, U.S.A.). Microfluidic traps and nanofluidic columns packed with Symmetry C18 (5 μm, 180 μm × 20 mm) were utilized for online trapping and desalting, and nanofluidic columns packed with BEH130 C18 (1.7 μm, 100 μm × 100 mm) were employed in analytical separation. The mobile phases purchased from Thermo Fisher Scientific (U.S.A.) were composed of water/acetonitrile/formic acid (A: 98/2/0.1%; B: 2/98/0.1%). A portion of a 2.25 μg (9 μL) sample was loaded, trapped, and desalted at a flow rate of 2 μL/min for 15 min with buffer A. Peptides were then separated using the following gradient at a flow rate of 300 nL/min: 5% B for 1 min, 5% to 35% B for 40 min, 35% to 80% B for 5 min, and 80% B for 5 min. Initial chromatographic conditions were restored after 2 min.

Data acquisition was performed with a TripleTOF 5600 System (AB SCIEX, USA) fitted with a Nanospray III source (AB SCIEX, USA). Data were acquired using an ion spray voltage of 2.5 kV. Survey scans were acquired in 250 ms, and up to 30 product ion scans were collected if they exceeded a threshold of 120 counts per second (counts/s) with a 2+ to 5+ charge-state. A sweeping collision energy setting of 35 ± 5 eV coupled with iTRAQ adjusted rolling collision energy was applied to all precursor ions for collision-induced dissociation. Dynamic exclusion was set for half of the peak width (18 s), and the precursor was then refreshed off the exclusion list.

Database Search and Quantification

The resulting MS/MS spectra were combined into one Mascot generic format (MGF) file and searched against the International Protein Index (IPI) mouse sequence databases (version 3.87, MOUSE, 59534 sequences) with MASCOT software (Matrix Science, London, U.K.; version 2.3.02). Only unique peptides used for protein quantification were chosen to quantify proteins. The search parameters were as follows: trypsin as the enzyme, with one missed cleavage allowed; a fixed modification of carbamidomethylation at Cys; variable modifications of oxidation at Met and iTRAQ 8-plex at Tyr; mass tolerance of 0.05 Da for peptide and 0.1 Da for fragment ions. An automatic decoy database search strategy was employed to estimate the false discovery rate (FDR). In the final search results, the FDR was less than 1.5%. iTRAQ 8-plex was chosen for quantification during the search. For protein identification, the filters were set as follows: significance threshold $p < 0.05$ (with 95% confidence) and ion score or expected cutoff less than 0.05 (with 95% confidence). For protein quantification, the filters were set as follows: "median" was chosen for protein ratio type; minimum precursor charge was set to 1, and minimum peptides were set to 2; only unique peptides were used to quantify proteins. Summed intensities were set as normalization, and outliers were removed automatically. The peptide threshold was set as above for identity threshold.

Because iTRAQ quantification underestimated "real" fold change between samples,[26] a protein with ≥1.2-fold difference and a p-value ≤0.05 was regarded as being differentially expressed in the data, as used in previous studies.[27−29]

Gene Ontology (GO) annotation of the identified proteins was done by searching the GO Web site (http://www.geneontology.org). GO terms enrichment analysis of the differentially expressed proteins was done with Cytoscape and its plugin BiNGO (version 2.3),[30] which is a java-based tool used to determine which GO categories are statistically over- or under-represented in a set of genes. To better understand these differentially expressed proteins in relation to published literature, interactions among these proteins regarding biological pathways were determined using Pathway Studio software via the ResNet database (version 6.5, Ingenuity Systems, Inc.).

Histopathological Examination

Three testes from each group were fixed in 10% Bouin's fixative and processed sequentially in ethanol, xylene, and paraffin. Tissues were then embedded in paraffin, sectioned (5 μm), and stained with hematoxylin and eosin (H&E).

Immunofluorescence Analysis

Cross sections (5 μm) of paraffin-embedded testes from control, 1.25, 5, and 20 mg PFOA/kg/d groups were deparaffinized, rehydrated, heated in 10 mM sodium citrate, and blocked using 0.5% BSA (wt/vol) for 30 min, followed by overnight incubation with primary antibodies (rabbit antimouse cytochrome P450 cholesterol side-chain cleavage enzyme (CYP11A1), insulin like-factor 3 (INSL3), Millipore Corp., Billerica, MA)) diluted in blocking solution (1:200) at 4 °C. After incubation, slides were washed three times with PBST and then incubated at room temperature for 1 h with Alexa Fluor-conjugated goat antirabbit IgG secondary antibodies (ZSGB-BIO; green fluorescence, Alexa Fluor 488) at 1:200 diluted with corresponding blocking solution. After washing three times with PBST, the sections were mounted with Vectorshield Antifade media with 4′,6-diamidino-2-phenyl-indole (DAPI, for staining cell nucleus) (ZSGB-BIO) for fluorescent microscopy. Fluorescent images were captured using a Nikon DS-Ris digital camera interface to a Nikon Eclipse 90i Fluorescence Microscope at 12.5-Megapixel (Mpx) with Nikon NIS Elements Advanced Research Imaging Software (Version 3.2) (Nikon Instruments Inc.). Images were exported to TIFF format and analyzed in Photoshop using Adobe Creative Suite (Version CS6).

Terminal Deoxynucleotidyl Transferase-Mediated Digoxigenin-Deoxyuridine Triphosphate Nick End Labeling (TUNEL)

Sections of testes from control, 1.25, 5, and 20 mg PFOA/kg/d groups were deparaffinized, hydrated, and immersed in Proteinase K for 10 min at room temperature. After washing with PBS for 15 min, treatment with 3% H_2O_2 for 10 min followed, and then the samples were rinsed with PBS for another 15 min. The sections were incubated with an In Situ Cell Death Detection Kit, POD (Peroxidase; Roche Applied Science) following the manufacturer's instructions, and the TUNEL-positive germ cells in the seminiferous tubules were counted. Three testis samples from each group were analyzed. Sixty tubules from each sample were counted.

Culture and Treatment of mLTC-1 cells

The mLTC-1 cells were purchased from the American Type Culture Collection (Manassas, VA) and cultured in RPMI 1640 medium containing 2.05 mM L-glutamine, 10% heat-inactivated fetal bovine serum, 100 IU/mL penicillin, and 100 g/mL streptomycin at 5% CO_2 and 37 °C. To assess the dose effects of PFOA, mLTC-1 cells were grown in culture to approximately 70% confluency, and fresh media containing increasing concentrations of PFOA (0−400 μM) were added
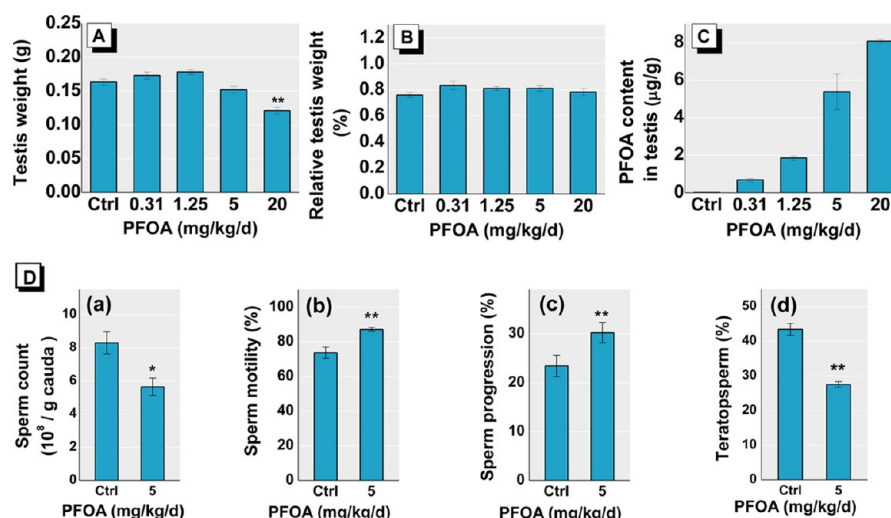
Figure 1. Effect of PFOA treatment on absolute testis weight ($n = 16$) (A) and relative testis weight ($n = 16$) (B), and testis PFOA content in male mice ($n = 3$) (C). Alteration in sperm number, sperm motility, progressiveness, teratosperm rate in male mice after treatment with PFOA (5 mg/kg/day) ($n = 5$) (D). Change (means $\pm$ SE) in sperm number (a), sperm motility (b), progressiveness (c), and teratosperm rate (d). Values are means $\pm$ SE ** $p < 0.01$ compared with control.

for 48 h. After 48 h exposure, cellular viability as the end point was determined using MTT assay. The inhibition of cellular viability (%) was calculated as Inhibition (%) = (1-OD$_{treated}$/OD$_{untreated}$) $\times$ 100%.

For progesterone determination, mLTC-1 cells were grown in culture to approximately 70% confluency and were then treated with fresh medium containing PFOA (0, 50, 100, 200, 300, and 400 μM) for 48 h. At the end of incubation, the medium was removed, and the cells were washed three times with PBS and stimulated for 3 h with cAMP (1 mM) or 22R-hydroxycholesterol (22R-HC, 50 μM) in serum-free medium. At the end of the 3 h incubation period, the cell medium was collected for progesterone determination, and the cells were dissolved in lysis buffer containing protease inhibitor PMSF for protein determination.

Western Blot Analysis

Western blot (WB) analysis was performed according to standard procedure.[31] Briefly, testes from control, 0.31, 1.25, 5, and 20 mg/kg/d group were lysed by RIPA buffer containing PMSF and phosphatase inhibitor cocktail (Sigma-Aldrich, St Louis, MO). A total of 20 μg protein from each sample was separated on 12.5% SDS-PAGE and then blotted onto a PVDF membrane (Millipore, Billerica, MA, USA). After blocking using nonfat milk (5%), the PVDF membranes were incubated with primary polyclonal antibodies including rabbit antimouse CYP11A1 (Millipore Corp., Billerica, MA), calreticulin (CALR) (Cell Signaling Technology, Inc., Danvers, MA), and steroidogenic acute regulatory protein (StAR) (Abcam Inc., Cambridge, MA). Antibody concentrations used were based on the manufacturer's specifications. After incubation with primary antibodies, the membranes were washed and incubated with an appropriate horseradish peroxidase (HRP)-conjugated secondary antibody (goat antirabbit IgG or rabbit antigoat IgG) (Boster Biological Technology, Wuhan, China). The protein bands were then visualized by enhanced chemiluminescence (superECL, Tigen, Beijing, China) on X-ray films and analyzed with QuantityOne Software (v 4.6.3, Bio-Rad). Data were normalized to protein expression levels of β-actin. Results were

presented as means $\pm$ SE for each experimental group of at least three individual samples.

Cholesterol and Hormones Determination

Total cholesterol (TCHO) content in the mice testes in the control and PFOA groups (0.31, 1.25, 5, and 20 mg/kg/d) were measured using commercial kits according to the manufacturer's instructions (Applygen Technologies, Beijing, China). Contents of testosterone and progesterone in the testes, progesterone in culture media, and serum luteinizing hormone (LH) were detected by radioimmunoassay (RIA) using commercial kits from the Beijing North Institute of Biological Technology, China. Testosterone, progesterone, and total cholesterol concentrations were normalized to testis protein concentration.

qPCR Analysis

Total RNA extraction and qPCR analysis were used to analyze samples from each group as described previously.[31] The mouse-specific primers for 10 genes involved in steroidogenesis and genes involved in cholesterol trafficking are given in SI. Mouse-specific primers are listed in Table S1 in the SI. β-actin was chosen as an internal control gene.

Statistical Analysis

Measurement data of testis weight, relative testis weight, testis lipid levels, testis testosterone and progesterone levels, qPCR analysis, and Western blot analysis were analyzed using SPSS for Windows 13.0 Software (SPSS, Inc., Chicago, IL) and were presented as means with standard errors (means $\pm$ SE). Differences between the control and treatment groups were detected using one-way analysis of variance (ANOVA), followed by Duncan's multiple range tests. A p-value of ≤ 0.05 was considered statistically significant.

■ RESULTS

Effect of PFOA on Testicular Weights, Sperm Quality, and Testicular Microstructures

Compared with the control group, absolute testis weight was significantly diminished only in the highest PFOA-dosed group (20 mg PFOA/kg/d) ($p < 0.01$) (Figure 1A); however, none of
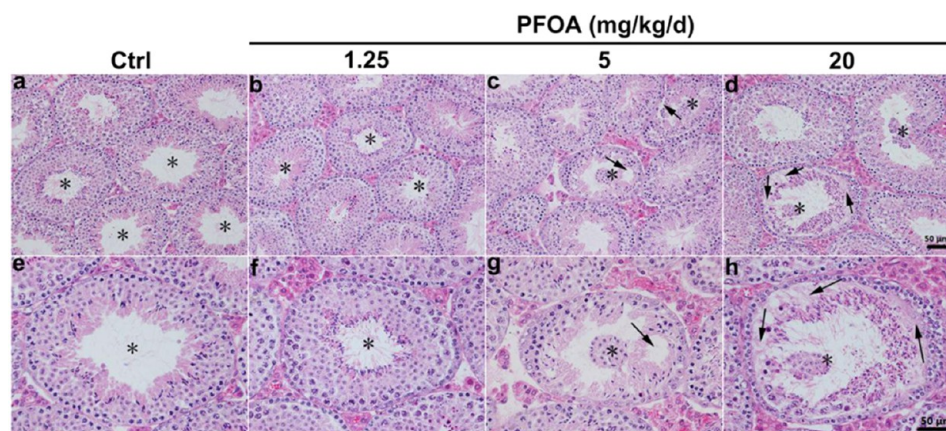
Figure 2. Effects of PFOA on seminiferous tubules (STs) under light microscopy. Normal histological structure in the control (a and e). Asterisks indicate tubular lumen (a, 200 × ; e, 400 ×). (b and f) Slightly atrophied shape of STs in 1.25 mg/kg/d PFOA group (b, 200 × ; f, 400 ×). (c and g) Badly damaged tubules and disorganized shape of seminiferous epithelium in 5 mg/kg/d PFOA group (c, 200 × ; g, 400 ×). (d and h) Severely damaged tubules and atrophied shape of seminiferous epithelium in 20 mg/kg/d PFOA group. (d, 200 × ; h, 400 ×). Arrow indicates lack of germ or Sertoli cells between basal membrane and adluminal portions. Bar = 50 μm.

the PFOA doses significantly altered testis weight relative to body weight (Figure 1B). Furthermore, correlations between external PFOA exposure and testis PFOA levels were analyzed. The PFOA levels in the testes increased in a dose-dependent manner after PFOA treatment. The PFOA level in the control was 0.01 μg/g wet weight, whereas they were 5.37 and 8.06 μg/g wet weight in the 5 and 20 mg PFOA/kg/d groups, showing a 537- and 806-fold increase, respectively, compared with the control (Figure 1C). We analyzed sperm quality in the epididymis. Epididymal sperm numbers were significantly lower in the PFOA-treated groups than in the control (Figure 1D, a). Sperm motility and progressiveness were significantly reduced compared with the control (Figure 1D, b and c). However, the teratospermia ratio (including head, neck, and tail teratospermia) was remarkably elevated in the PFOA-exposed groups compared with the control (Figure 1D, d and Figure S1 in the SI).

Testicular morphology was evaluated to investigate structural damage in the mouse testis induced by PFOA. The testes in the control group exhibited normal histological features, and the seminiferous tubules showed spermatogenic activity with successive stages of spermatogonia to spermatozoa transformation. The germ cells were organized in concentric layers, and the tubular lumens were empty (Figure 2a and e). There were no significant morphometric differences between the control and the low-dose treatment group (0.31 and 1.25 mg/kg/d) (Figure 2b and f, and Figure S2 in the SI). However, the seminiferous epithelia in the seminiferous tubules were severely atrophied, with large numbers of germ cell deficiencies between the basal membrane and adluminal portions (Figure 2c, d, g, and h) in the high PFOA dose groups (5 and 20 mg/kg/d). In addition, detached germ cells were sloughed off into the tubular lumen. These results indicated that PFOA damaged the seminiferous tubules.

Differentially Expressed Protein Identification and Relative Quantification by iTRAQ Analysis

Three individual samples were included in the iTRAQ experiment from the control and 5 mg PFOA/kg/d group. The MS/MS analysis identified a total of 191,833 mass spectra. After data filtering to exclude low-scoring spectra, 16,494 unique spectra matched to special peptides were obtained.

Searching using Mascot version 2.3.02 identified a total of 8,369 unique peptides from 2,868 proteins (Table S2, in the SI). In our iTRAQ data, the coverage levels of all biological replicates were between 94% and 98% when the cutoff point was at ±50% variation (Table S3, in the SI), which showed good repeatability among the three biological replicates of each group. Expression differences greater than 1.2-fold and an abundance change threshold of 20% together with a p-value <0.05 were applied to classify protein interests and potential significance for future hypotheses and investigations. Results showed that 93 proteins (52 up-regulated and 41 down-regulated) were significantly differentially expressed after 5 mg/kg/d PFOA treatment (Table 1).

Calreticulin (CALR) is related to cell proliferation and spermatogenesis[32] and with a 1.29-fold increase in the 5 mg/kg/d PFOA group, as determined by iTRAQ analysis, and was selected for validation using WB. Interestingly, in all validations, the average differences in the CALR expression levels as determined by WB analysis were greater than those from iTRAQ analysis (Figure S3 in the SI). This was similar to previous findings that iTRAQ quantification usually underestimates the "real" fold change between samples.[26]

Bioinformatics Analysis for Differential Expressed Proteins Induced by PFOA

Gene Ontology data including molecular function, cellular localization and biological processes (Table S4 in the SI) of the differentially expressed proteins were analyzed and sorted. The GO categories were ranked by their corrected (Corr) p-value, which indicated the degree of overrepresentation in the significantly differentially expressed proteins compared with the complete *Mus musculus* proteome (Figure S4 in the SI). The most overrepresented functions in the GO molecular functions category were involved with binding to targets (67 proteins), such as lipids, nucleic acid, proteins, ions, and steroids. For example, nine proteins (including apolipoprotein A1 (APOA1), fatty acid binding protein, adipocyte (FABP4), CYP11A1, and annexin A5 (ANXA5)) were related with lipid binding, which was significantly overrepresented with a corrected p-value of 6.7×10^{-5} (Figure S4A in the SI). In addition, the most significantly overrepresented biological processes were cell processes including cell metabolic

Table 1. Lists of Differential Expressed Proteins Identified by iTRAQ[a] in Mouse Testis after 5 mg/kg/day PFOA Exposure for 28 Days

accession	gene symbol	full name	ratio (P/C)[b]	QuaPep[c]	function description
IPI00110487	2310003C23Rik	Protein C20orf11 homologue	1.206	2	–
IPI00403329	2310008H09Rik	Protein C16orf88 homologue isoform 3	1.401	2	–
IPI00894788	2610019F03Rik	Uncharacterized protein	0.747	4	–
IPI00229804	Acbd5	Isoform 3 of Acyl-CoA-binding domain-containing protein 5	0.817	2	Lipid transport
IPI00317309	Anxa5	Annexin A5	0.79	4	Inhibition of blood coagulation
IPI00121209	Apoa1	Apolipoprotein A-I	0.505	14	Lipid transport
IPI00170307	Apoa1bp	Apolipoprotein A-I-binding protein	1.201	4	Lipid transport
IPI00349069	B230208H17Rik	Putative GTP-binding protein Parf	0.685	2	Signal transduction
IPI00119959	Banf1	Barrier-to-autointegration factor	1.347	17	DNA integration
IPI00115553	BC005624	Uncharacterized protein C9orf78 homologue	0.824	2	–
IPI00130950	Bhmt	Betaine–homocysteine S-methyltransferase 1	0.679	9	Amino acid metabolism
IPI00410791	Brd3	Isoform 1 of Bromodomain-containing protein 3	0.691	5	Transcription regulation
IPI00123639	Calr	Calreticulin	1.288	24	Cell differentiation, spermatogenesis
IPI00135186	Calu	Calumenin	0.75	5	Platelet activation
IPI00221890	Car3	Carbonic anhydrase 3	0.646	4	Response to oxidative stress
IPI00123755	Cbx5	Chromobox protein homologue 5	0.825	6	Transcription regulation
IPI00229310	Cdc34	Ubiquitin-conjugating enzyme E2 R1	1.231	8	Protein metabolism, cell cycle
IPI00229604	Cherp	Calcium homeostasis endoplasmic reticulum protein	0.785	5	Cell proliferation, calcium homeostasis
IPI00114409	Clta	Clathrin light chain A	0.821	6	Protein transport
IPI00222188	Col1a2	Collagen alpha-2(I) chain	0.792	21	Signal transduction
IPI00129571	Col3a1	Collagen alpha-1(III) chain	0.769	6	Organ development
IPI00262488	Crip1	Cysteine-rich protein 1	0.775	3	Apoptotic process, cell proliferation
IPI00118825	Csl	Citrate synthase-like protein	1.208	4	Citrate metabolism
IPI00136928	Cyp11a1	Cholesterol side-chain cleavage enzyme, mitochondrial	0.696	3	Progesterone biosynthetic process
IPI00133708	D1 Pas1	Putative ATP-dependent RNA helicase Pl10	1.259	5	Spermatogenesis, cell proliferation
IPI00113781	Dbil5	Diazepam-binding inhibitor-like 5	1.344	8	Lipid transport, spermatogenesis
IPI00308222	Dbnl	Isoform 2 of Drebrin-like protein	0.72	6	Signal transduction, adaptive immunity
IPI00123922	Ddc8	Differential display clone 8	1.38	2	Spermatogenesis
IPI00944009	Eef1d	Isoform 3 of Elongation factor 1-delta	1.233	4	Translation
IPI00226872	Efhd2	Uncharacterized protein	0.744	18	–
IPI00129276	Eif3a	Eukaryotic translation initiation factor 3 subunit A	0.8	15	Translation
IPI00187443	Eif5	Eukaryotic translation initiation factor 5	0.803	9	RNA metabolism
IPI00316509	Ephx1	Epoxide hydrolase 1	0.573	5	Stress response
IPI00116705	Fabp4	Fatty acid-binding protein, adipocyte	0.726	10	Fatty acid metabolism, transport
IPI00230139	Fkbp4	Peptidyl-prolyl cis–trans isomerase FKBP4	1.204	14	Steroid hormone receptor complex assembly
IPI00404590	H 1f0	Putative uncharacterized protein	1.63	8	Nucleosome assembly, DNA fragmentation
IPI00319916	H1fnt	Testis-specific H1 histone	1.549	5	Chromosome condensation
IPI00153399	Haus1	HAUS augmin-like complex subunit 1	1.267	3	Cell division
IPI00116442	Hdgfrp2	Isoform 3 of Hepatoma-derived growth factor-related protein 2	0.804	10	Transcription
IPI00224067	Hdgfrp3	Isoform 1 of Hepatoma-derived growth factor-related protein 3	0.761	4	Cell proliferation
IPI00123379	Hdlbp	Vigilin	0.664	3	Lipid transport cholesterol metabolism
IPI00223713	Hist1h1c	Histone H1.2	1.496	5	Chromatin organization, nucleosome assembly
IPI00319556	Hist1h1t	Histone H1t	1.38	20	Spermatogenesis, sperm motility
IPI00989397	Hist1h2al	src substrate cortactin	1.605	19	Inflammatory response
IPI00111957	Hist1h2ba	Histone H2B type 1-A	1.315	6	Nucleosome assembly, inflammatory response
IPI00114642	Hist1h2bj	Histone H2B type 1-F/J/L	1.286	8	Nucleosome assembly
IPI00309322	Hmox2	Heme oxygenase 2	1.2	8	Ion transport, stress response
IPI00133916	Hnrnph1	Heterogeneous nuclear ribonucleoprotein H	1.246	15	RNA metabolism
IPI00230449	Hpcal1	Hippocalcin-like protein 1	0.563	4	Calcium ion binding
IPI00123802	Hsph1	Isoform HSP105-alpha of Heat shock protein	0.816	2	Stress response
IPI00133417	Ifit3	Interferon-induced protein with tetratricopeptide repeats 3	0.686	3	Apoptosis, virus response
IPI00114234	Insl3	Insulin-like 3	0.736	3	Sex differentiation, gonad development
IPI00129356	Itsn1	Isoform 1 of Intersectin-1	0.774	3	Signal transduction
IPI00312076	Kif3a	Uncharacterized protein	1.316	3	Cytoskeleton

Table 1. continued

accession	gene symbol	full name	ratio (P/C)[b]	QuaPep[c]	function description
IPI00229527	Lta4h	Leukotriene A-4 hydrolase	1.25	6	Inflammatory response, amino acid metabolism
IPI00112346	Mapk14	Isoform 1 of Mitogen-activated protein kinase 14	1.2	2	Signal transduction, glucose metabolism
IPI00348435	Mex3d	RNA-binding protein MEX3D	1.287	7	Nucleic acid metabolism
IPI00113259	Mgarp	Uncharacterized protein C4orf49 homologue	0.822	2	Stress response
IPI00111831	Naca	Nascent polypeptide-associated complex subunit alpha, muscle-specific form	1.275	10	Transcription
IPI00330551	Ndufaf2	Mimitin, mitochondrial	0.828	7	Oxidation−reduction process
IPI00224128	Nmt1	Glycylpeptide N-tetradecanoyltransferase 1	1.34	4	Lipoprotein metabolism, embryonic development
IPI00406365	Nt5c1b	Isoform 1 of Cytosolic 5∼nucleotidase 1B	1.213	2	Nucleotide metabolism
IPI00309704	Nucb2	Nucleobindin-2	0.82	15	Calcium ion homeostasis
IPI00121018	Ogfr	Isoform 1 of Opioid growth factor receptor	0.808	6	Growth regulation
IPI00224740	Pfn1	Profilin-1	1.365	7	Cytoskeleton
IPI00131960	Pole4	DNA polymerase epsilon subunit 4	0.811	2	Transcription
IPI00221454	Prdx6 ps1	Peroxiredoxin 6, related sequence 1	1.416	8	Stress response
IPI00115257	Psip1	Isoform 1 of PC4 and SFRS1-interacting protein	1.219	3	Stress response
IPI00137831	Rcn1	Reticulocalbin-1	0.786	3	Calcium ion binding
IPI00133185	Rpl14	60S ribosomal protein L14	1.387	5	Translation
IPI00263879	Rpl35	60S ribosomal protein L35	1.202	2	Translation
IPI00313222	Rpl6	60S ribosomal protein L6	1.514	20	Translation
IPI00137787	Rpl8	60S ribosomal protein L8	1.38	4	Translation
IPI00121427	S100a6	Protein S100-A6	0.638	5	Cell division, signal transduction
IPI00134131	Scp2	Isoform SCPx of Nonspecific lipid-transfer protein	0.761	5	Lipid transport and metabolism, cell proliferation
IPI00123920	Serpina1c	Alpha-1-antitrypsin 1−3	0.32	4	Acute phase response
IPI00131830	Serpina3k	Serine protease inhibitor A3K	0.262	27	Acute phase response
IPI00116105	Serpina6	Corticosteroid-binding globulin	2.004	3	Transport, glucocorticoid metabolism
IPI00454140	Skiv2l	Superkiller viralicidic activity 2-like	0.702	2	mRNA splicing
IPI00134191	Slc2a3	Solute carrier family 2, facilitated glucose transporter member 3	1.205	8	Carbohydrate transport and metabolism
IPI00108041	Stim1	Stromal interaction molecule 1	0.803	6	Detection of calcium ion
IPI00115321	Stk10	Serine/threonine-protein kinase 10	0.75	4	Protein metabolism
IPI00466570	Tmed10	Isoform 1 of Transmembrane emp24 domain-containing protein 10	1.351	3	Protein transport
IPI00309878	Tpd52l1	Uncharacterized protein	0.752	3	Apoptosis
IPI00623570	Trip12	Thyroid hormone receptor interactor 12	0.801	3	DNA repair
IPI00274407	Tufm	Isoform 1 of Elongation factor Tu, mitochondrial	1.211	9	Protein biosynthesis
IPI00125652	Txn2	Thioredoxin, mitochondrial	0.722	3	Stress response
IPI00129516	Uqcrh	Cytochrome b-c1 complex subunit 6, mitochondrial	0.717	5	Electron transport
IPI00122547	Vdac2	Voltage-dependent anion-selective channel protein 2	1.252	7	Ion transport
IPI00409127	Wdr62	WD repeat-containing protein 62	1.271	2	Cerebral cortex development
IPI00221569	Zadh2	Zinc-binding alcohol dehydrogenase domain-containing protein 2	0.814	3	Oxidation−reduction process
IPI00421162	Zc3h11a	Zinc finger CCCH domain-containing protein 11A	0.791	4	Zinc ion binding
IPI00648513	Zc3h18	Isoform 1 of Zinc finger CCCH domain-containing protein 18	0.795	4	Zinc ion binding

[a]The iTRAQ was performed on three biological replicates. [b]The iTRAQ ratios (P/C) were based on the median value from three biological replicates in both control (C) and PFOA (P) exposed groups. A protein with ≥1.2-fold difference and a p-value ≤0.05 was regarded as being differentially expressed. [c]QuaPep: peptide number used for protein quantification.

processes, organelle organization and translation (Figure S4B in the SI). Four proteins (vigilin (HDLBP), APOA1, CYP11A1, and corticosteroid binding globulin (SERPINA6)) were annotated with steroid metabolism with a corrected p-value of 0.029.

Using Pathway Studio software analysis, ten proteins (e.g., FABP4, CALR, insulin like-factor 3 (INSL3), APOA1, and CYP11A1) were related to lipid and steroid metabolism directly or indirectly (Figure 3A). Many proteins were found to be associated with germ cell processes, such as apoptosis, cell

survival, cell proliferation, and spermatogenesis (Figure 3B). For example, a total of 32 proteins, including CALR, carbonic anhydrase 3 (CAR3), leukotriene A4 hydrolase (LTA4H) and mimitin, mitochondrial (NDUFAF2), were related to cell proliferation. Additionally, 28 proteins, such as thioredoxin, mitochondrial (TXN2), isoform heat shock protein 105 kD alpha (HSPH1), epoxide hydrolase 1 (EPHX1), and HAUS augmin-like complex, subunit 1 (HAUS1), were related to apoptosis. Thus, the occurrences of testicular germ cell apoptosis were analyzed. In the PFOA-treated groups, the

Figure 3. Analysis of regulatory network of all differentially expressed proteins identified in the mice testes. Pathway analysis was performed using Pathway Studio (v 7.0) software. (A) Network of proteins related to lipid and steroid metabolism. (B) Network of germ cell processes.

number of apoptotic germ cells detected by TUNEL increased in a dose-dependent manner (Figure 4A and B). In contrast, TUNEL-positive cells were rare in the control group. The apoptotic germ cells formed after exposure to PFOA were mostly restricted to the spermatogonia, and other types of germ cells in the spermatogenic lineage appeared intact. In addition,

TUNEL-positive staining was not detected in other testicular cell types (e.g., Leydig cells or Sertoli cells) in any group.

Effect of PFOA on Leydig Cell Function

Leydig cells play a vital role in maintaining proper levels of male hormones, including testosterone. In this study, damage to Leydig cell microstructure was not observed by HE staining or

Figure 4. Incidence of apoptotic germ cell death after treatment with PFOA for 28 days. (A) TUNEL staining of testes (original magnification, 100 ×, bar = 50 μm for a−d, and 400 ×, bar = 25 μm for e−h). Arrow indicates apoptosis of spermatocyte, and arrowhead indicates apoptosis of round germ cells. (B) TUNEL-positive germ cells were quantitatively analyzed by total positive cells per seminiferous tubule. Sixty tubules in each testis were counted. Values are means ± SE (n = 3). ** $p < 0.01$ and *** $p < 0.001$ compared with control.
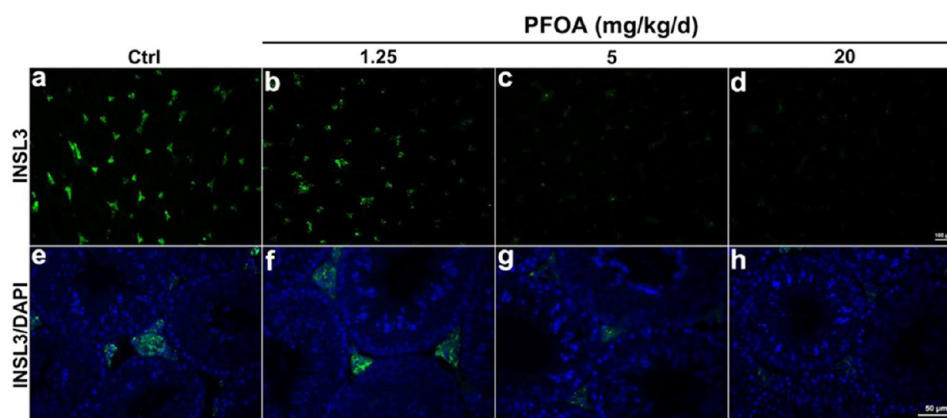
Figure 5. Immunolocalization of INSL3 in Leydig cells of mice treated with vehicle (controls) or PFOA. Green fluorescence represents abundant INSL3, blue fluorescence shows nuclei stained with DAPI. (a, b, e, f) INSL3 immunostaining was bright in clusters of interstitial cells. (c, d, g, h) immunoexpression of INSL3 significantly declined. Bars = 100 μm for a−d and 50 μm for e−h.

apoptosis analysis. However, iTRAQ analysis showed decreased levels of two Leydig-cell-specific marker proteins (INSL3 and CYP11A1) (Table 1). Immunohistochemical analysis was used to show the effects of PFOA exposure on the expression of INSL3 proteins in Leydig cells (Figure 5). Exposure to PFOA resulted in the down regulation of INSL3 expression in a dose−response manner.

CYP11A1 is a mitochondrial enzyme that catalyzes conversion of cholesterol to pregnenolone in Leydig cells. This is the first reaction in steroidogenesis in Leydig cells. Figure 6 shows the effects of PFOA exposure on the expression of CYP11A1 in the testes. Exposure to PFOA resulted in the down-regulation of CYP11A1 expression in a dose-dependent manner, as shown by Western blotting (Figure 6A and B) and

RT-PCR (Figure 6C). We further confirmed these observations by immunolocalization of the testicular sections (Figure 6D).

We next determined the contents of testosterone and progesterone as well as their precursor cholesterol in the testes. Significant decreases in testosterone and progesterone were observed after PFOA exposure ($p < 0.05$) (Figure 7A and B). Testosterone content in the 5 mg PFOA/kg/d group was about 48% that of the control, and was reduced to 0.1 μg/g in the 20 mg/kg/d group, far below that in the control. Total cholesterol content in the testes also decreased significantly in the 5 and 20 mg PFOA/kg/d groups ($p < 0.05$) (Figure 7C).

Synthesis of testosterone takes place via the actions of 3β-hydroxysteroid dehydrogenase (3β-HSD), 17α-hydroxy/C17−20lase (CYP17A1), and 17β-hydroxysteroid dehydrogenase
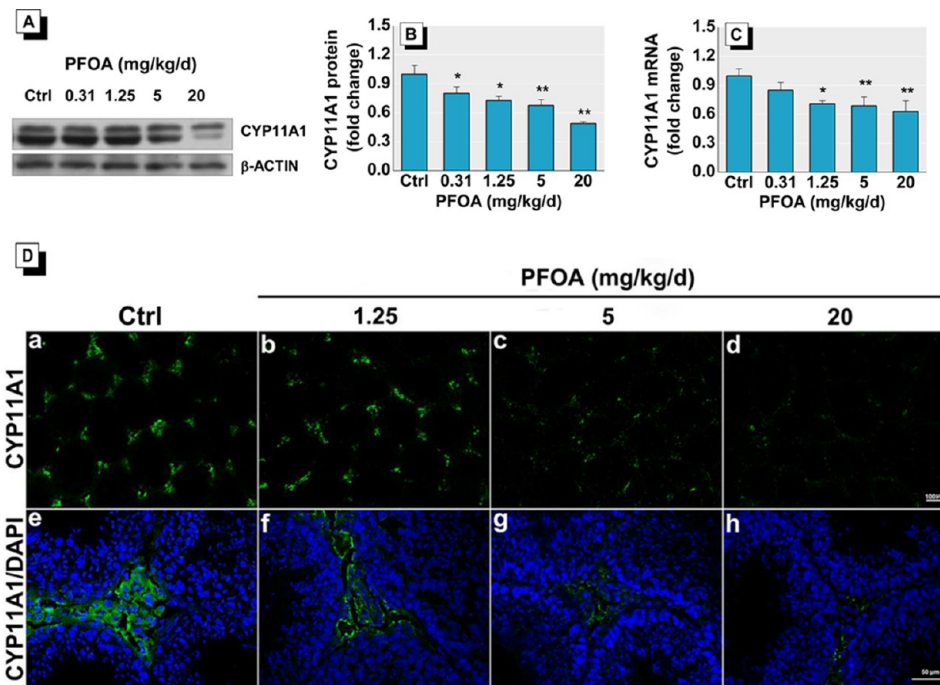
Figure 6. CYP11A1 expression and localization in testicular interstitial compartments of mice treated with PFOA. (A) Western blot analysis for CYP11A1 in different PFOA groups. (B) Mean levels of protein bands compared with the control. Values are means ± SE of three mice per group. (C) Quantitative real-time PCR analysis for gene expressions of CYP11A1 levels in mice testes. (D) Immunolocalization of CYP11A1 in testicular interstitial compartments of mice treated with PFOA. (a, b, e, f) CYP11A1 immunostaining was bright in clusters of interstitial cells; (c, d, g, h) immunoexpression of CYP11A1 significantly decreased. Bars = 100 μm for a−d and 50 μm for e−h. Data are means ± SE ($n = 3$), * $p < 0.05$, ** $p < 0.01$ compared with control.
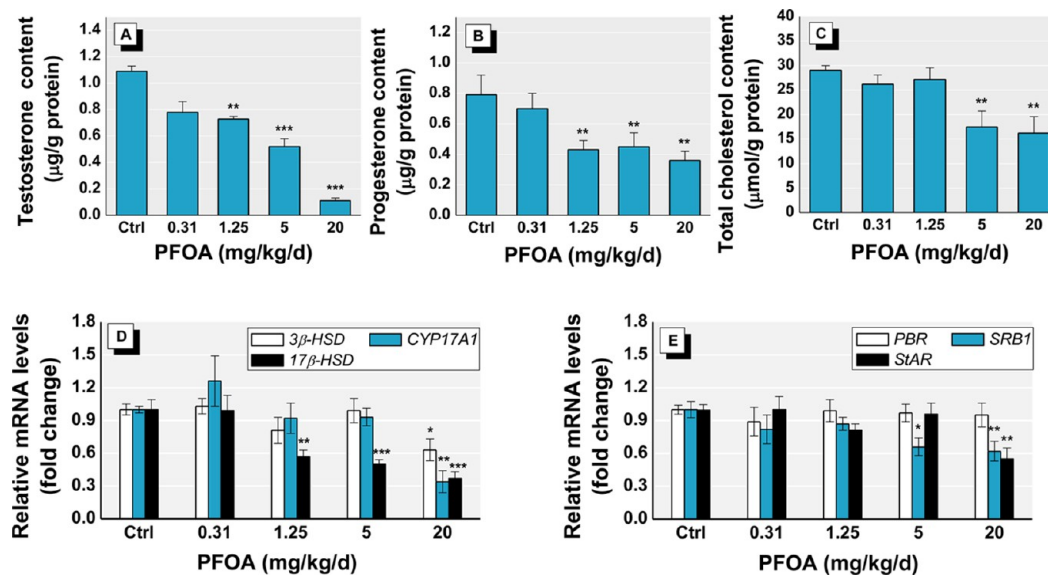
Figure 7. Effects of PFOA on testosterone (A), progesterone (B), and total cholesterol contents (C), transcriptionally expressed levels of genes involved in testosterone biosynthesis (D) and transferring cholesterol (E) in mice testes. β-Actin was used as the housekeeping gene. Data are means ± SE ($n = 6$) * $p < 0.05$, ** $p < 0.01$; *** $p < 0.001$ compared with control.

(17β-HSD). Compared with the control, transcriptional expressions of 3β-HSD and CYP17A1 decreased significantly in the highest dose group. However, transcriptional expression of 17β-HSD decreased significantly after treatment with doses of 1.25, 5, and 20 mg PFOA/kg/d (Figure 7D).

Since the total amount of cholesterol decreased in the testes in the 5 and 20 mg PFOA/kg/d groups, the effects of PFOA exposure on transcriptionally expressed levels of genes involved

in transferring cholesterol to the testes were investigated. Compared with the control group, transcriptional expressions of scavenger receptor B1 (SRB1) involved in transporting plasma cholesterol to steroidogenic tissues showed significant decrease in the 5 and 20 mg PFOA/kg/d groups ($p < 0.01$). Levels of steroidogenic acute regulatory protein (StAR), which is responsible for cholesterol transport to the inner mitochondrial membrane, were significantly reduced only at
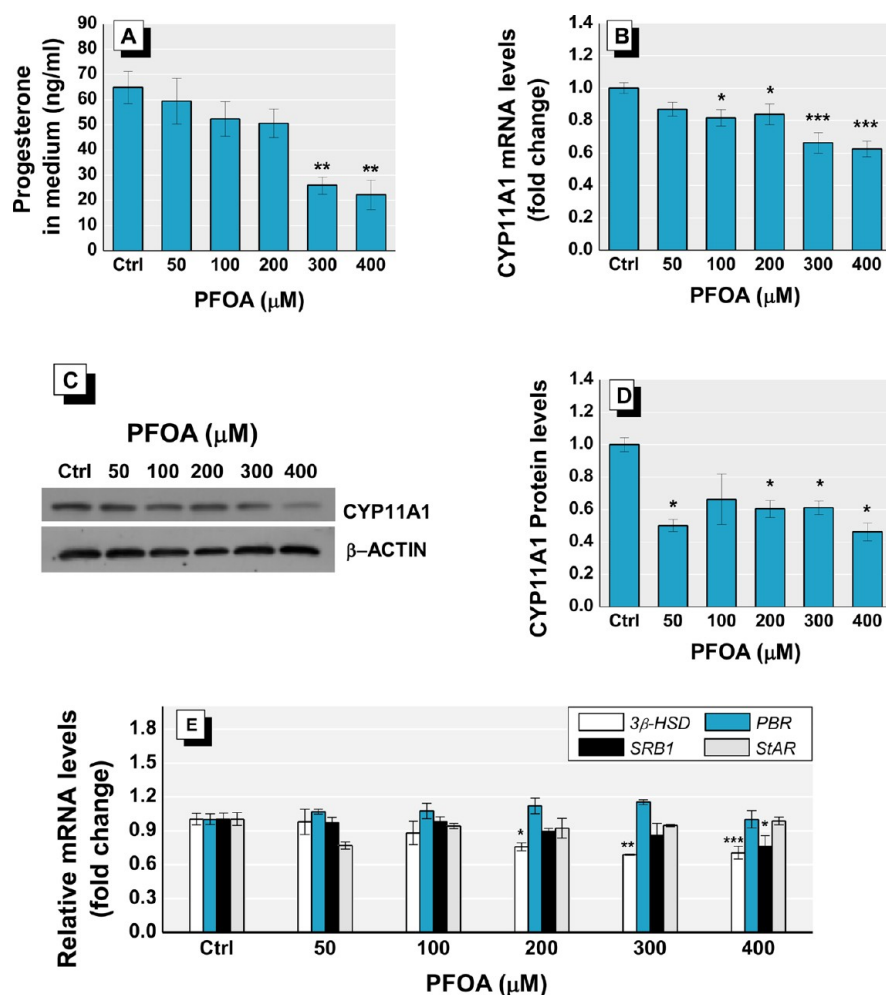
Figure 8. Effects of PFOA on progesterone (A), transcriptionally expressed levels of CYP11A1 (B), protein levels of CYP11A1 by Western blot analysis (C) and quantification of CYP11A1 in protein levels (D), and transcriptionally expressed levels of genes involved in steroidogenesis-related genes in cAMP-treated mLTC-1 cells. Following 3 h of cAMP stimulation, mLTC-1 cells were treated with PFOA for 48 h. Data are means ± SE (n = 3) from three independent experiments in triplicate. * $p < 0.05$, ** $p < 0.01$; and *** $p < 0.001$* compared with control.

doses of 20 mg PFOA/kg/d ($p < 0.01$) (Figure 7E). In contrast, transcriptional expressions of the peripheral-type benzodiazepine receptor (PBR) did not change at any dose of PFOA. In addition, transcriptional expressions of 3-hydroxy-3-methyl-glutaryl-CoA reductase and hydroxymethylglutaryl-CoA synthase, which are important enzymes in cholesterol *de novo* synthesis, did not change after PFOA treatment (Figure S5 in the SI).

We next measured the LH concentrations in serum and the transcriptionally expressed levels of its receptor (LHR) in the testes. No significant change in serum LH levels or LHR transcriptional expression levels were observed in the testes after PFOA exposure (Figure S6 in the SI).

Effects of PFOA on CYP11A1 Expression and Product of Progesterone in mLTC-1 Cells

MTT assay was used to assess the cellular toxicity of PFOA, and the results showed that cell viability was not affected by PFOA (0−400 μM) (Figure S7 in the SI). In addition, PFOA inhibited cAMP-induced progesterone synthesis in mLTC-cells in a dose-dependent manner (Figure 8A). Interestingly, exposure to PFOA resulted in the down-regulation of CYP11A1 expression, as shown by RT-PCR at 100−400 μM PFOA (Figure 8B) and Western blotting (Figure 8C and D). In

contrast, no statistical differences in transcriptional expression of PBR, SRB1, and StAR were observed in the experimental concentrations of PFOA, except for SRB1 at 400 μM PFOA ($p < 0.05$) (Figure 8E). Compared with the control, however, transcriptional expression of 3β-HSD decreased significantly at 200−400 μM PFOA.

To examine whether PFOA inhibited steroidogenesis by inhibiting CYP11A1 expression directly, mLTC-1 cells were treated with 200 μM of PFOA for 24 h and then incubated with 50 μM of 22R-HC for 3 h. 22R-HC freely enters the inner mitochondrial membrane without the help of a transporter. Treatment with 22R-HC resulted in a 2.6-fold increase in progesterone levels relative to untreated cells (Figure 9A). However, PFOA significantly inhibited 22R-HC-stimulated progesterone production in mLTC-1 cells (Figure 9A). In particular, PFOA significantly inhibited CYP11A1 protein levels in 22R-HC-stimulated cells but did not affect StAR protein levels (Figure 9B−D).

■ DISCUSSION

PFOA is a suspected endocrine disruptor, which affects sex hormones resulting in lower testosterone and higher estradiol levels.[12,13,19,20] The influence of PFOA on the male reproductive system was reviewed by Kennedy[11] and Lau et
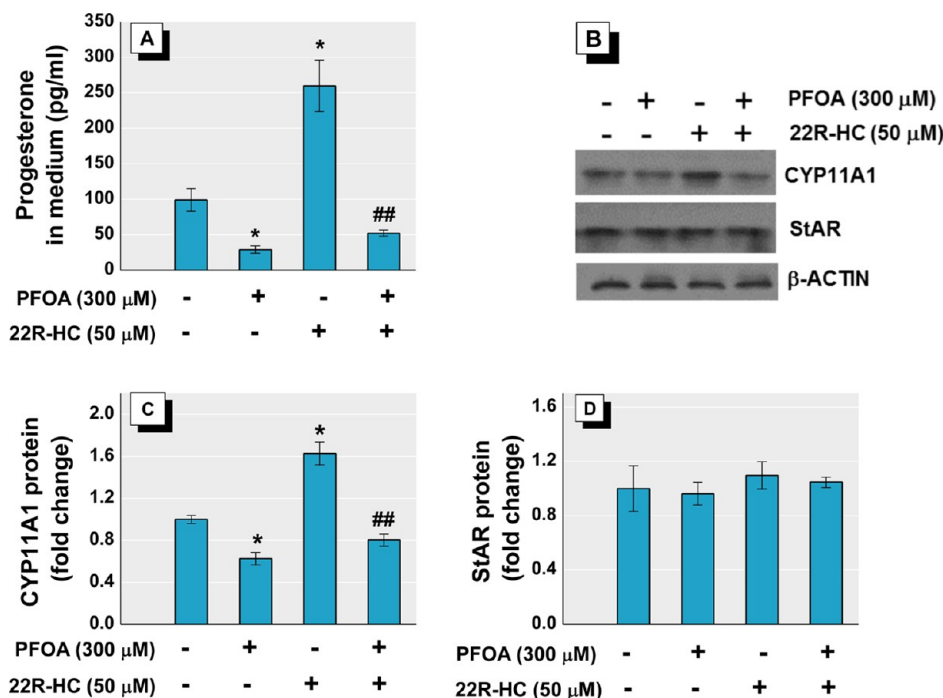
Figure 9. Effects of PFOA on progesterone production (A), protein levels of CYP11A1 and StAR by Western blot analysis (B), quantification of CYP11A1 (C) and StAR (D) in protein levels in mLTC-1 cells treated with 22R-HC. mLTC-1 cells were treated with 300 μM PFOA for 48 h and then stimulated with 50 μM 22R-HC for 3 h. Data are means $\pm$ SE (n = 3) from three independent experiments in triplicate. * $p < 0.05$, compared with untreated control. ## $p < 0.01$, compared with 22R-HC group.

al.,[33] and mainly focused on toxicities to the F1 or F2 generations. Studies on testicular toxicity of PFOA are limited, and the mode of action is not well-known. In addition to measuring classic toxicology indexes, we conducted an in-depth proteomic analysis to provide global information regarding the potential mode of action for PFOA.

After 28 days of PFOA treatment, the relative testis weight of treated mice did not change significantly compared with that of the control, which was similar to previous studies on ammonium perfluorooctanoate.[13] The decrease in absolute testis weight in the 20 mg PFOA/kg/d group might be due to a significant decrease in body weight by PFOA,[34] which suggested that a general toxicity of PFOA might have occurred in this dose. In addition, PFOA content in the testes increased in a dose-dependent manner, similar to changes in serum PFOA concentrations.[34] The PFOA content in the testes of the 20 mg PFOA group reached 8.06 μg/g, and the corresponding serum PFOA content was 105 μg/mL, which was similar to the highest serum PFOA levels reported in PFOA production workers. The PFOA serum elimination half-life in workers was estimated up to 3.8 years, much longer than the days for male rats or mice to weeks for monkeys.[6] Considering the obvious toxicity of PFOA on the structure and function of the mouse testis when the exposure dose was above 1.25 mg/kg/d, testis toxicity of PFOA on humans, especially occupational workers, needs further attention.

The primary function of testosterone is to stimulate spermatogenesis (sperm production) and support the development of immature spermatozoa (sperm). Thus, an abnormal reduction in intratesticular fluid testosterone can cause testicular atrophy, which is accompanied by a decrease in the number of germ cells and, ultimately, azoospermia. In the present study, obvious structural lesions in the testes induced by oral exposure to PFOA were observed through histopatho-

logical examination. In some seminiferous tubules (STs), the germ cells underwent a loss of adhesion to the Sertoli cells (SC) and sloughed off into the lumen of the STs. In the PFOA-treated groups, in particular, the number of apoptotic germ cells detected by TUNEL increased in a dose-dependent manner. These results showed a direct effect of PFOA on the mouse testis. A similar phenomenon was also observed in male rats exposed to PFNA and PFDoA, showing features of apoptosis in SC and germ cells.[19,20] However, the mechanism of testicular damage in mice induced by PFCAs has not yet been clarified. Some studies reported that degeneration of STs was associated with decreasing testosterone concentrations.[35−37] In the present study, the levels of intratesticular testosterone were reduced significantly at doses of 1.25, 5, and 20 mg PFOA/kg/d, as were testicular progesterone levels. A dose-dependent decrease in testosterone production was observed in hCG-stimulated Leydig cells treated *in vitro* with ammonium perfluorooctanoate, but *in vivo* experiments showed no changes in serum or testicular testosterone levels.[13] Similar inhibition of testosterone levels by PFOA were also reported on isolated rat Leydig cells.[14] These results all suggest that PFOA can induce functional lesions in the testis, and inhibit testosterone synthesis.

To uncover the global proteomic alteration in the mouse testis after PFOA treatment, iTRAQ analysis was conducted. Considering obvious histopathological changes occurred in the 5 and 20 mg/kg/d-dosed groups and significant decrease of body weight in 20 mg/kg/d,[34] testes from control and 5 mg/kg/d group were chosen for iTRAQ analysis. Ninety-three proteins which differed in expression level were identified. Using bioinformatics analysis, it was found that among these proteins, a total of 28 were related to apoptosis. Additionally, 32 proteins were predicted to be associated with cell proliferation, and some with cell survival, cell development,

chromatin remodeling, and spermatogenesis. Moreover, 10 proteins were predicted to be related to lipid and steroid metabolism either directly or indirectly. These proteins might help explain the structural and functional damage in mice testes induced by PFOA.

In the present study, ANXA5 was found to be related to apoptosis, cell survival, and cell proliferation through Pathway Studio analysis. ANXA5 belongs to a huge family of evolutionary-related annexin proteins and is often used for detecting early-stage apoptotic cells. One of its major physiological roles is as a modulator of the immune response by inhibiting phagocytosis during clearance of apoptotic and necrotic cells.[38] Additionally, several studies have reported that overexpression of ANXA5 stimulated apoptosis in growth plate chondrocytes,[39] inhibited sperm production in male infertility,[40] and was up-regulated in normozoospermic patients with infertility.[41] In our study, however, ANXA5 was down-regulated in mouse testes after PFOA exposure, which was inconsistent with the apoptosis phenomenon found in TUNEL analysis. Animal studies have suggested that apoptosis is a key regulator of spermatogenesis as a mechanism to delete superfluous or defective germ cells.[40,42] ANXA5 was also found to gradually decrease in relative abundance in germ cells during spermatogenesis, with higher protein levels in spermatogonia than that in pachytene spermatocytes and early spermatids.[43] Thus, we speculated that the decrease in ANXA5 here might contribute to the effect of PFOA on cell types of spermatogenesis. In addition, whether ANXA5 plays a role in cell−cell communication among cells in the testis after PFOA exposure is unclear and needs further investigation.

In our study, INSL3 was associated with apoptosis, spermatogenesis, cell proliferation, as well as steroid metabolism. INSL3 is a major secreted product of interstitial Leydig cells in all male mammals, and can activate G protein-coupled receptor−relaxin family peptide receptor 2 (RFPR2) to prevent male germ cell apoptosis.[44] Del Borgo et al.[45] showed that intratesticular injection of an INSL3 antagonist led to substantial germ cell loss, pointing to INSL3 having an antiapoptotic function. Moreover, a clinical study showed that serum INSL3 was positively correlated with sperm concentration at the end of testosterone treatment and was significantly associated with nonazoospermia.[46] Higher serum INSL3 concentrations were associated with persistent sperm production, indicating that INSL3 may play a role in preventing complete suppression of spermatogenesis in some men on hormonal contraceptive regimens.[46] Thus, we speculated that the lower INSL3 expression observed in PFOA-treated mice may influence the spermatogenesis function of the testes. PFOS has been shown to reduce the epididymal sperm count in mice.[45−48] Additionally, circulating INSL3 concentrations in humans[49,50] and rats[51] reflect the differentiation status and number of Leydig cells present. Therefore, the decrease in INSL3 protein levels in the present study suggested that PFOA exposure could lead to a reduction in or malfunction of the mouse LC population.

Testosterone is essential for germ cell survival, apoptosis, and development in the testis.[37,52] One important role of LCs is to synthesize testosterone through a series of reactions catalyzed by four enzymes: CYP11A1, 3β-HSD, CYP17A1, and 17β-HSD. As an LC specific marker, CYP11A1 converts cholesterol to pregnenolone, which is the first rate-limiting and hormonally regulated step in the synthesis of all steroid hormones. In the present study, CYP11A1 was reduced significantly at the

mRNA and protein levels in the mice testes in a dose-dependent manner. Furthermore, *in vitro* study showed that the reduction in progesterone levels was also accompanied by decreased expression of CYP11A1 in cAMP-stimulated mLTC-1 cells. Previous studies showed a decrease in testosterone levels in isolated rat Leydig cells with PFOA treatment.[13,14] However, exposure to PFOA caused no change in testosterone, progesterone, or gene expression levels of CYP11A in the human H295R adrenocortical carcinoma cell line.[53,54] This discrepancy between *in vitro* effects on testosterone synthesis in human and rat cells might be species specific. The reduced testicular steroid production, including progesterone and testosterone, in the PFOA-treated groups suggested that the steroidogenesis function of LCs in mice were dramatically damaged by PFOA, and CYP11A1 might be a target and main contributing factor.

In the present study, the mRNA expression level of 17β-HSD was reduced significantly in 1.25, 5, and 20 mg/kg/d groups and a dose-dependent effect was observed. However, the mRNA levels of 3β-HSD, CYP17A1 and 17β-HSD gene level decreased significantly in 20 mg/kg/d group, which might be due to the general toxicity of PFOA or the sequential change after a decrease of CYP11A levels. Similarly, the activities of 3β-HSD and 17β-HSD were also inhibited by PFOA in primary rat LCs, corresponding with a reduction in testosterone production.[14] However, whether the inhibitions of 3β-HSD, CYP17A1, and 17β-HSD after PFOA exposure are associated with a decrease in CYP11A1 remain uncertain.

Additionally, testosterone production is highly regulated via negative feed-back control of the hypothalamic−pituitary−testicular (HPT) axis and primary luteinizing hormone (LH) acting on steroidogenic enzymes and steroid transport proteins. For example, StAR expression can be stimulated via LH binding to its receptor (LHR).[55,56] To confirm whether the decreased testosterone was related to the direct inhibition of neuro-endocrine function by PFOA, we analyzed the changes in serum LH levels and transcriptional levels in the testes. However, our results showed no obvious changes in the serum LH levels and mRNA levels of LHR in the testes of the PFOA-treated groups compared with the control, suggesting that the inhibition of steroidogenesis in mice by PFOA was independent of the HPG axis.

Cholesterol is a substrate for testosterone biosynthesis. LCs can employ several potential sources of cholesterol for steroidogenesis and *de novo* synthesis in the endoplasmic reticulum (ER), including cholesterol stored in lipid droplets as cholesterol esters, uptake of circulating HDL via scavenger receptor B1 (SRB1), and uptake of LDL via receptor-mediated endocytosis. In mice, HDL-derived selective uptake of cholesteryl esters, via SRB1, provides most of the cholesterol for steroidogenesis, with lesser contributions from LDL and *de novo* synthesis, which differs from humans and other mammals.[57,58] In the present study, SRB1 and StAR were inhibited at the mRNA levels after 5 and 20 mg/kg/d PFOA exposure. These results were similar to our previous studies conducted on rats exposed to acute PFDoA,[20] which suggested that PFCAs could decrease testosterone biosynthesis with a concomitant reduction in the expression of key genes responsible for cholesterol transport.

Considering that testicular cholesterol levels decreased significantly in the 5 and 20 mg/kg/d PFOA groups, and serum cholesterol levels decreased in a dose-dependent manner in our previous study,[34] we cannot exclude that the decrease in

serum cholesterol induced by PFOA was the initial cause of testicular testosterone reduction. In our *in vitro* studies, PFOA significantly inhibited 22R-HC-stimulated progesterone production in mLTC-1 cells, and was accompanied by a significant decrease in CYP11A1 protein levels, but no effect on StAR protein levels. This indicated that PFOA might inhibit progesterone production by inhibiting CYP11A1 directly, regardless of intracellular cholesterol content. However, whether the expression levels of SRB1, 3β-HSD, and CYP11A were inhibited by PFOA directly or inhibited as a sequential occurrence of the decrease in cholesterol levels remains unclear and needs further *in vitro* study.

In summary, our data indicate that exposure to PFOA resulted in damage to the seminiferous tubules, increased spermatogonial apoptosis, and decreased testosterone levels in the testes. We used iTRAQ to identify 93 differentially expressed proteins involved in steroid metabolism, spermatogenesis, and apoptosis. Analyzing these interactions allowed us to characterize the down-regulated expression of CYP11A1 as a Leydig-cell-specific marker. Our study suggested that PFOA exposure disturbed testosterone levels and that CYP11A1 might be a major steroidogenic enzyme targeted by PFOA.

ASSOCIATED CONTENT

Supporting Information

Detailed information about sperm quality and PFOA analysis methods; qPCR primers used in this study; elementary proteomics data revealed by iTRAQ; biological reproducibility of iTRAQ analysis; GO analysis of differentially expressed proteins; raw data for all proteins and peptides identified using iTRAQ; teratosperm rate in mouse treated by PFOA; Western blot validation of calreticulin (CALR) protein levels in mice testes after PFOA treatment; overview of GO Slim generic distribution of differentially expressed proteins; mRNA levels of HMG-CoA R and HMG-CoA S in the testis after PFOA treatment; LH levels in mouse serum (A) and its transcriptionally expressed levels in the testis as well as in cAMP-treated mLTC-1 cells after PFOA treatment; and concentration–response relationship for the inhibitory effect of PFOA on mLTC-1 cells. This material is available free of charge via the Internet at http://pubs.acs.org.

AUTHOR INFORMATION

Corresponding Author

***Corresponding Author** Tel.: +86-(0)10-64807085. Fax: +86-(0)10-64807099. E-mail: daijy@ioz.ac.cn.

Author Contributions

[#]H.Z. and Y.L. contributed equally to this work.

Notes

The authors declare no competing financial interest.

ACKNOWLEDGMENTS

REFERENCES

(1) 3M, The Leader in Electrofluorination. In *3M Company Technical Bulletin*; 3M Company: St. Paul, MN, 1995.

(2) Holzapfel, W. Uses of Fluorinated Surfactants. *Fette, Seifen, Anstrichm.* **1966**, *68*, 837−842.

(3) Giesy, J. P.; Kannan, K. Perfluorochemical surfactants in the environment. *Environ. Sci. Technol.* **2002**, *36* (7), 146A−152A.

(4) Rotander, A.; Karrman, A.; van Bavel, B.; Polder, A.; Riget, F.; Auethunsson, G. A.; Vikingsson, G.; Gabrielsen, G. W.; Bloch, D.; Dam, M. Increasing levels of long-chain perfluorocarboxylic acids (PFCAs) in Arctic and North Atlantic marine mammals, 1984−2009. *Chemosphere* **2012**, *86* (3), 278−285.

(5) Brantsaeter, A. L.; Whitworth, K. W.; Ydersbond, T. A.; Haug, L. S.; Haugen, M.; Knutsen, H. K.; Thomsen, C.; Meltzer, H. M.; Becher, G.; Sabaredzovic, A.; Hoppin, J. A.; Eggesbo, M.; Longnecker, M. P. Determinants of plasma concentrations of perfluoroalkyl substances in pregnant Norwegian women. *Environ. Int.* **2013**, *54*, 74−84.

(6) Lau, C.; Anitole, K.; Hodes, C.; Lai, D.; Pfahles-Hutchens, A.; Seed, J. Perfluoroalkyl acids: a review of monitoring and toxicological findings. *Toxicol. Sci.* **2007**, *99* (2), 366−394.

(7) Olsen, G. W.; Burris, J. M.; Burlew, M. M.; Mandel, J. H. Plasma cholecystokinin and hepatic enzymes, cholesterol and lipoproteins in ammonium perfluorooctanoate production workers. *Drug Chem. Toxicol.* **2000**, *23* (4), 603−620.

(8) Lou, I.; Wambaugh, J. F.; Lau, C.; Hanson, R. G.; Lindstrom, A. B.; Strynar, M. J.; Zehr, R. D.; Setzer, R. W.; Barton, H. A. Modeling single and repeated dose pharmacokinetics of PFOA in mice. *Toxicol. Sci.* **2009**, *107* (2), 331−341.

(9) Seals, R.; Bartell, S. M.; Steenland, K. Accumulation and clearance of perfluorooctanoic acid (PFOA) in current and former residents of an exposed community. *Environ. Health Perspect.* **2011**, *119* (1), 119−124.

(10) Biegel, L. B.; Hurtt, M. E.; Frame, S. R.; O'Connor, J. C.; Cook, J. C. Mechanisms of extrahepatic tumor induction by peroxisome proliferators in male CD rats. *Toxicol. Sci.* **2001**, *60* (1), 44−55.

(11) Kennedy, G. L., Jr.; Butenhoff, J. L.; Olsen, G. W.; O'Connor, J. C.; Seacat, A. M.; Perkins, R. G.; Biegel, L. B.; Murphy, S. R.; Farrar, D. G. The toxicology of perfluorooctanoate. *Crit. Rev. Toxicol.* **2004**, *34* (4), 351−384.

(12) White, S. S.; Fenton, S. E.; Hines, E. P. Endocrine disrupting properties of perfluorooctanoic acid. *J. Steroid Biochem. Mol. Biol.* **2011**, *127* (1−2), 16−26.

(13) Biegel, L. B.; Liu, R. C.; Hurtt, M. E.; Cook, J. C. Effects of ammonium perfluorooctanoate on Leydig cell function: *in vitro*, *in vivo*, and *ex vivo* studies. *Toxicol. Appl. Pharmacol.* **1995**, *134* (1), 18−25.

(14) Zhao, B.; Chu, Y.; Hardy, D. O.; Li, X. K.; Ge, R. S. Inhibition of 3beta- and 17beta-hydroxysteroid dehydrogenase activities in rat Leydig cells by perfluorooctane acid. *J. Steroid Biochem. Mol. Biol.* **2010**, *118* (1−2), 13−17.

(15) Wei, Y.; Dai, J.; Liu, M.; Wang, J.; Xu, M.; Zha, J.; Wang, Z. Estrogen-like properties of perfluorooctanoic acid as revealed by expressing hepatic estrogen-responsive genes in rare minnows (*Gobiocypris rarus*). *Environ. Toxicol. Chem.* **2007**, *26* (11), 2440−2447.

(16) Benninghoff, A. D.; Bisson, W. H.; Koch, D. C.; Ehresman, D. J.; Kolluri, S. K.; Williams, D. E. Estrogen-like activity of perfluoroalkyl acids *in vivo* and interaction with human and rainbow trout estrogen receptors *in vitro*. *Toxicol. Sci.* **2011**, *120* (1), 42−58.

(17) Zhao, B.; Hu, G. X.; Chu, Y.; Jin, X.; Gong, S.; Akingbemi, B. T.; Zhang, Z.; Zirkin, B. R.; Ge, R. S. Inhibition of human and rat 3beta-hydroxysteroid dehydrogenase and 17beta-hydroxysteroid dehydrogenase 3 activities by perfluoroalkylated substances. *Chem. Biol. Interact.* **2010**, *188* (1), 38−43.

(18) Feng, Y.; Fang, X.; Shi, Z.; Xu, M.; Dai, J. Effects of PFNA exposure on expression of junction-associated molecules and secretory function in rat Sertoli cells. *Reprod. Toxicol.* **2010**, *30* (3), 429−437.

(19) Feng, Y.; Shi, Z.; Fang, X.; Xu, M.; Dai, J. Perfluorononanoic acid induces apoptosis involving the Fas death receptor signaling pathway in rat testis. *Toxicol. Lett.* **2009**, *190* (2), 224−230.

(20) Shi, Z.; Zhang, H.; Liu, Y.; Xu, M.; Dai, J. Alterations in gene expression and testosterone synthesis in the testes of male rats exposed to perfluorododecanoic acid. *Toxicol. Sci.* **2007**, *98* (1), 206−215.

(21) Joensen, U. N.; Bossi, R.; Leffers, H.; Jensen, A. A.; Skakkebaek, N. E.; Jorgensen, N. Do perfluoroalkyl compounds impair human semen quality? *Environ. Health Perspect.* **2009**, *117* (6), 923−927.

(22) Vested, A.; Ramlau-Hansen, C. H.; Olsen, S. F.; Bonde, J. P.; Kristensen, S. L.; Halldorsson, T. I.; Becher, G.; Haug, L. S.; Ernst, E. H.; Toft, G. Associations of *in utero* exposure to perfluorinated alkyl acids with human semen quality and reproductive hormones in adult men. *Environ. Health Perspect.* **2013**, *121* (4), 453−458 458e451−455..

(23) Raymer, J. H.; Michael, L. C.; Studabaker, W. B.; Olsen, G. W.; Sloan, C. S.; Wilcosky, T.; Walmer, D. K. Concentrations of perfluorooctane sulfonate (PFOS) and perfluorooctanoate (PFOA) and their associations with human semen quality measurements. *Reprod. Toxicol.* **2012**, *33* (4), 419−427.

(24) Son, H. Y.; Kim, S. H.; Shin, H. I.; Bae, H. I.; Yang, J. H. Perfluorooctanoic acid-induced hepatic toxicity following 21-day oral exposure in mice. *Arch. Toxicol.* **2008**, *82* (4), 239−246.

(25) Bao, J.; Jin, Y.; Liu, W.; Ran, X.; Zhang, Z. Perfluorinated compounds in sediments from the Daliao River system of northeast China. *Chemosphere* **2009**, *77* (5), 652−657.

(26) Karp, N. A.; Huber, W.; Sadowski, P. G.; Charles, P. D.; Hester, S. V.; Lilley, K. S. Addressing accuracy and precision issues in iTRAQ quantitation. *Mol. Cell. Proteomics* **2010**, *9* (9), 1885−1897.

(27) Moulder, R.; Lonnberg, T.; Elo, L. L.; Filen, J. J.; Rainio, E.; Corthals, G.; Oresic, M.; Nyman, T. A.; Aittokallio, T.; Lahesmaa, R. Quantitative proteomics analysis of the nuclear fraction of human CD4+ cells in the early phases of IL-4-induced Th2 differentiation. *Mol. Cell. Proteomics* **2010**, *9* (9), 1937−1953.

(28) Duthie, K. A.; Osborne, L. C.; Foster, L. J.; Abraham, N. Proteomics analysis of interleukin (IL)-7-induced signaling effectors shows selective changes in IL-7Ralpha449F knock-in T cell progenitors. *Mol. Cell. Proteomics* **2007**, *6* (10), 1700−1710.

(29) Auer, J.; Camoin, L.; Guillonneau, F.; Rigourd, V.; Chelbi, S. T.; Leduc, M.; Laparre, J.; Mignot, T. M.; Vaiman, D. Serum profile in preeclampsia and intra-uterine growth restriction revealed by iTRAQ technology. *J. Proteomics* **2010**, *73* (5), 1004−1017.

(30) Maere, S.; Heymans, K.; Kuiper, M. BiNGO: a Cytoscape plugin to assess overrepresentation of gene ontology categories in biological networks. *Bioinformatics* **2005**, *21* (16), 3448−3449.

(31) Zhang, H.; Ding, L.; Fang, X.; Shi, Z.; Zhang, Y.; Chen, H.; Yan, X.; Dai, J. Biological responses to perfluorododecanoic acid exposure in rat kidneys as determined by integrated proteomic and metabonomic studies. *PLoS One* **2011**, *6* (6), e20862.

(32) Zhu, N.; Pewitt, E. B.; Cai, X.; Cohn, E. B.; Lang, S.; Chen, R.; Wang, Z. Calreticulin: An intracellular Ca++-binding protein abundantly expressed and regulated by androgen in prostatic epithelial cells. *Endocrinology* **1998**, *139* (10), 4337−4344.

(33) Lau, C.; Butenhoff, J. L.; Rogers, J. M. The developmental toxicity of perfluoroalkyl acids and their derivatives. *Toxicol. Appl. Pharmacol.* **2004**, *198* (2), 231−241.

(34) Yan, S.; Wang, J.; Zhang, W.; Dai, J. Circulating microRNA profiles altered in mice after 28 days exposure to perfluorooctanoic acid. *Toxicol. Lett.* **2013**, *224*, 24−31.

(35) Kim, J. M.; Ghosh, S. R.; Weil, A. C.; Zirkin, B. R. Caspase-3 and caspase-activated deoxyribonuclease are associated with testicular germ cell apoptosis resulting from reduced intratesticular testosterone. *Endocrinology* **2001**, *142* (9), 3809−3816.

(36) Sinha Hikim, A. P.; Rajavashisth, T. B.; Sinha Hikim, I.; Lue, Y.; Bonavera, J. J.; Leung, A.; Wang, C.; Swerdloff, R. S. Significance of apoptosis in the temporal and stage-specific loss of germ cells in the adult rat after gonadotropin deprivation. *Biol. Reprod.* **1997**, *57* (5), 1193−1201.

(37) Young, K. A.; Nelson, R. J. Mediation of seasonal testicular regression by apoptosis. *Reproduction* **2001**, *122* (5), 677−685.

(38) Munoz, L. E.; Frey, B.; Pausch, F.; Baum, W.; Mueller, R. B.; Brachvogel, B.; Poschl, E.; Rodel, F.; von der Mark, K.; Herrmann, M.; Gaipl, U. S. The role of annexin A5 in the modulation of the immune response against dying and dead cells. *Curr. Med. Chem.* **2007**, *14* (3), 271−277.

(39) Wang, W.; Kirsch, T. Annexin V/beta5 integrin interactions regulate apoptosis of growth plate chondrocytes. *J. Biol. Chem.* **2006**, *281* (41), 30848−30856.

(40) Maeda, Y.; Shiratsuchi, A.; Namiki, M.; Nakanishi, Y. Inhibition of sperm production in mice by annexin V microinjected into seminiferous tubules: possible etiology of phagocytic clearance of apoptotic spermatogenic cells and male infertility. *Cell Death Differ.* **2002**, *9* (7), 742−749.

(41) Xu, W.; Hu, H.; Wang, Z.; Chen, X.; Yang, F.; Zhu, Z.; Fang, P.; Dai, J.; Wang, L.; Shi, H.; Li, Z.; Qiao, Z. Proteomic characteristics of spermatozoa in normozoospermic patients with infertility. *J. Proteomics* **2012**, *75* (17), 5426−5436.

(42) Print, C. G.; Loveland, K. L. Germ cell suicide: New insights into apoptosis during spermatogenesis. *BioEssays* **2000**, *22* (5), 423−430.

(43) Rolland, A. D.; Evrard, B.; Guitton, N.; Lavigne, R.; Calvel, P.; Couvet, M.; Jegou, B.; Pineau, C. Two-dimensional fluorescence difference gel electrophoresis analysis of spermatogenesis in the rat. *J. Proteome Res.* **2007**, *6* (2), 683−697.

(44) Kawamura, K.; Kumagai, J.; Sudo, S.; Chun, S. Y.; Pisarska, M.; Morita, H.; Toppari, J.; Fu, P.; Wade, J. D.; Bathgate, R. A.; Hsueh, A. J. Paracrine regulation of mammalian oocyte maturation and male germ cell survival. *Proc. Natl. Acad. Sci. U.S.A.* **2004**, *101* (19), 7323−7328.

(45) Del Borgo, M. P.; Hughes, R. A.; Bathgate, R. A.; Lin, F.; Kawamura, K.; Wade, J. D. Analogs of insulin-like peptide 3 (INSL3) B-chain are LGR8 antagonists *in vitro* and *in vivo*. *J. Biol. Chem.* **2006**, *281* (19), 13068−13074.

(46) Amory, J. K.; Page, S. T.; Anawalt, B. D.; Coviello, A. D.; Matsumoto, A. M.; Bremner, W. J. Elevated end-of-treatment serum INSL3 is associated with failure to completely suppress spermatogenesis in men receiving male hormonal contraception. *J. Androl.* **2007**, *28* (4), 548−554.

(47) Wan, H. T.; Zhao, Y. G.; Wong, M. H.; Lee, K. F.; Yeung, W. S.; Giesy, J. P.; Wong, C. K. Testicular signaling is the potential target of perfluorooctanesulfonate-mediated subfertility in male mice. *Biol. Reprod.* **2011**, *84* (5), 1016−1023.

(48) Qiu, L.; Zhang, X.; Zhang, X.; Zhang, Y.; Gu, J.; Chen, M.; Zhang, Z.; Wang, X.; Wang, S. Sertoli cell is a potential target for perfluorooctane sulfonate (PFOS)- induced reproductive dysfunction in male. *Toxicol. Sci.* **2013**, *135*, 229−240.

(49) Foresta, C.; Bettella, A.; Vinanzi, C.; Dabrilli, P.; Meriggiola, M. C.; Garolla, A.; Ferlin, A. A novel circulating hormone of testis origin in humans. *J. Clin. Endocrinol. Metab.* **2004**, *89* (12), 5952−5958.

(50) Anand-Ivell, R.; Wohlgemuth, J.; Haren, M. T.; Hope, P. J.; Hatzinikolas, G.; Wittert, G.; Ivell, R. Peripheral INSL3 concentrations decline with age in a large population of Australian men. *Int. J. Androl.* **2006**, *29* (6), 618−626.

(51) Anand-Ivell, R.; Heng, K.; Hafen, B.; Setchell, B.; Ivell, R. Dynamics of INSL3 peptide expression in the rodent testis. *Biol. Reprod.* **2009**, *81* (3), 480−487.

(52) Walker, W. H. Molecular mechanisms of testosterone action in spermatogenesis. *Steroids* **2009**, *74* (7), 602−607.

(53) Rosenmai, A. K.; Nielsen, F. K.; Pedersen, M.; Hadrup, N.; Trier, X.; Christensen, J. H.; Vinggaard, A. M. Fluorochemicals used in food packaging inhibit male sex hormone synthesis. *Toxicol. Appl. Pharmacol.* **2013**, *266* (1), 132−142.

(54) Liu, C.; Zhang, X.; Chang, H.; Jones, P.; Wiseman, S.; Naile, J.; Hecker, M.; Giesy, J. P.; Zhou, B. Effects of fluorotelomer alcohol 8:2 FTOH on steroidogenesis in H295R cells: Targeting the cAMP signalling cascade. *Toxicol. Appl. Pharmacol.* **2010**, *247* (3), 222−228.

(55) Dufau, M. L. Endocrine regulation and communicating functions of the Leydig cell. *Annu. Rev. Physiol.* **1988**, *50*, 483−508.

(56) Zirkin, B. R.; Chen, H. Regulation of Leydig cell steroidogenic function during aging. *Biol. Reprod.* **2000**, *63* (4), 977−981.

(57) Miller, W. L.; Bose, H. S. Early steps in steroidogenesis: Intracellular cholesterol trafficking. *J. Lipid Res.* **2011**, *52* (12), 2111−2135.

(58) Azhar, S.; Reaven, E. Scavenger receptor class BI and selective cholesteryl ester uptake: Partners in the regulation of steroidogenesis. *Mol. Cell. Endocrinol.* **2002**, *195* (1−2), 1−26.